

# On Achievable Gravimetric and Volumetric Energy Densities of Al Dual-Ion Batteries

Cite This: *ACS Energy Lett.* 2023, 8, 1266–1269

Read Online

ACCESS |

Metrics &amp; More

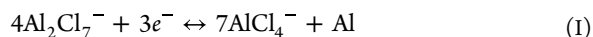
Article Recommendations

Supporting Information

Aluminum dual-ion batteries (ADIBs) are presently gaining attention as emerging stationary energy storage systems in view of their low cost,<sup>1</sup> long cycling life,<sup>2–4</sup> and high energy efficiency.<sup>5</sup> Seminal reports on intercalation of  $\text{AlCl}_4^-$  ions into graphite by Foulletier et al. date back to the 1970s.<sup>6</sup> The past decade has seen renewed and extensive research in this area, aiming at developing practical ADIBs.<sup>7,8</sup> These studies encompass the mechanisms of intercalation and diffusion of the  $\text{AlCl}_4^-$  ions in cathode materials,<sup>9</sup> the degree of the cathode volume expansion,<sup>10–12</sup> the electrochemical properties of ionic liquid electrolytes,<sup>13</sup> and so forth. While the underlying chemistries are now rather well understood, the literature thus far still lacks a balanced battery-level assessment of achievable gravimetric and volumetric energy densities. Since ADIBs are not rocking-chair-type batteries, like aluminum-ion or lithium-ion batteries, the approaches are not directly interchangeable, either. This Viewpoint aims to close this gap. Such analysis is particularly needed to guide engineering of the architecture of the battery, optimal loadings of cathode materials, and proportions of active and inactive components in the battery.

Typically, laboratory tests aim at the deliberate testing of ionic liquid electrolytes and cathode materials, thus using cells containing, for instance, a large excess of the ionic liquid electrolyte and active cathode material loadings. ADIBs vastly differ from Al-ion batteries. There is no one-directional movement of  $\text{Al}^{3+}$  ions through the electrolyte from the negative to the positive electrodes and vice versa. Instead, chloroaluminate ionic liquid acts as both the electrolyte and electrode material, and in the following it is referred to as the anolyte. It acts as a source of  $\text{Al}_2\text{Cl}_7^-$  and  $\text{AlCl}_4^-$  ions required for electrochemical energy storage in accordance with the following charge/discharge reactions:

On the negative electrode:



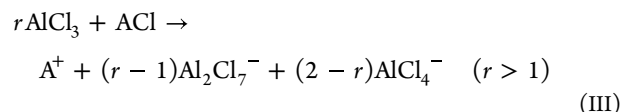
On the positive electrode:



where AM is a cathode active material.

A typical example of the anolyte is a mixture of  $\text{AlCl}_3$  (Lewis acid) and another organic ion chloride ( $\text{ACl}$ , Lewis base), such as 1-ethyl-3-methylimidazolium chloride (EMIMCl). As a result of the acid–base interactions, the salt mixture becomes a

liquid at room temperature and comprises  $\text{AlCl}_4^-$ ,  $\text{AlCl}_4^-/\text{Al}_2\text{Cl}_7^-$ , or  $\text{Al}_2\text{Cl}_7^-$  anions (depending on the molar ratio of  $\text{AlCl}_3/\text{ACl}$ ), which are charge-balanced by organic cations:



This anolyte serves for reversible plating/stripping of Al at the Al foil and acts as the source of  $\text{AlCl}_4^-$  ions required for the intercalation/insertion into the positive electrode during charge. The chemical composition and quantity of the anolyte are thus changing upon charge and discharge, contrary to “rocking-chair” Al-ion battery systems, where chloroaluminate ionic liquid acts solely as a transmitter of the  $\text{Al}^{3+}$  ions. The theoretical quantity of the anolyte is the one providing the needed quantity of  $\text{Al}_2\text{Cl}_7^-$  ions, because solely  $\text{Al}_2\text{Cl}_7^-$  ions enable the electroplating of aluminum.<sup>14,15</sup> The charging of ADIBs stops when no  $\text{Al}_2\text{Cl}_7^-$  ions are left in the ionic liquid, which results in the formation of the neutral melt ( $[\text{AlCl}_3]:[\text{Cl}^-] = 1$ ). Considering the concentration of  $\text{Al}_2\text{Cl}_7^-$  ions in an ionic liquid electrolyte, which can be expressed through the parameter  $r$  (“acidity”), which is the  $\text{AlCl}_3:\text{ACl}$  molar ratio, and molar masses  $M$  of  $\text{AlCl}_3$  and  $\text{ACl}$ , the charge storage capacity of the chloroaluminate ionic liquid electrolytes is<sup>16</sup>

$$\text{Gravimetric } C_{\text{an}} = \frac{Fx(r-1)}{rM_{\text{AlCl}_3} + M_{\text{ACl}}} \quad (\text{mAh g}^{-1}) \quad (\text{1})$$

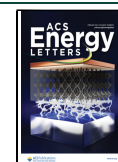
$$\text{Volumetric } C_{\text{an}} = \frac{Fx(r-1)\rho}{rM_{\text{AlCl}_3} + M_{\text{ACl}}} \quad (\text{mAh cm}^{-3}) \quad (\text{2})$$

where  $F = 26.8 \times 10^3 \text{ mAh mol}^{-1}$  (the Faraday constant),  $x = \frac{3}{4}$  (number of electrons required for reduction of 1 mol of the  $\text{Al}_2\text{Cl}_7^-$  ions),  $M_{\text{AlCl}_3}$  is the molar mass of  $\text{AlCl}_3$  in  $\text{g mol}^{-1}$ ,  $M_{\text{ACl}}$  is the molar mass of the  $\text{Cl}^-$  source (for example, EMIMCl) in  $\text{g mol}^{-1}$ ,  $r$  is the  $\text{AlCl}_3:\text{ACl}$  molar ratio ( $r > 1$ ),

Received: December 26, 2022

Accepted: January 24, 2023

Published: February 1, 2023



and  $\rho$  is density of the chloroaluminate-based anolyte in  $\text{mL}^{-1}$ .

We further calculate the achievable gravimetric and volumetric energy densities of ADIBs with graphite cathode<sup>5,17</sup> and EMIM anolyte,<sup>18</sup> with several assumptions as to the other components and size of the battery. Graphite thus far offers the most compelling characteristics as a cathode in terms of energy efficiency, charge-storage capacity, average discharge voltage, and reversibility when compared to other known ADIB cathode materials.<sup>8</sup> To account for the effects of anolyte acidity on the voltage and capacity of graphite, they were varied in the range of 1.77–2.02 V and 117–148  $\text{mAh g}^{-1}$  (245–311  $\text{mAh cm}^{-3}$ ), respectively. These values were determined experimentally when cycling Kish graphite flakes at a current density of 100  $\text{mA g}^{-1}$  using anolytes with different acidities.<sup>5</sup> We considered the conventional composition of the cathode, particularly, 97 wt% cathode active material and 3 wt% pVdF binder, although the contribution of the latter to the energy densities is rather small, as shown in Figure S1. The cathodes consisted of 30 vol% of pores which are filled with anolyte.

The quantity of the anolyte must at least match the charge of the used graphite (in  $\text{mAh}$ ). For instance, with the graphite and anolyte capacities of 100  $\text{mAh g}^{-1}$  and 48  $\text{mAh g}^{-1}$ , respectively, a 1  $\text{cm}^2$  graphite electrode with a capacity of 1  $\text{mAh cm}^{-2}$  (corresponding to a loading of 10  $\text{mg cm}^{-2}$ ) must be coated by 15  $\mu\text{L}$  of anolyte. The practical charge storage capacities of the anolyte are by ca. 10–14% lower at a current densities higher than 20  $\text{mA g}^{-1}$ .<sup>19</sup> We thus factored in the effect of varying the excess of anolyte on the resulting energy density of ADIBs. The excess of anolyte was also expressed as an N/P ratio, which is the ratio of the areal capacity of the anolyte (in  $\text{mAh cm}^2$ ) to the areal capacity of the graphite (in  $\text{mAh cm}^2$ ). Molybdenum cathode current collector (12  $\mu\text{m}$  thick foil) was used for the analysis, as its oxidative stability in highly corrosive chloroaluminate ionic liquids was demonstrated to be significantly higher than those of stainless steel, Al, Ti, and Ni.<sup>20</sup> The aluminum anode is comprised of 12  $\mu\text{m}$  thick Al foil.

The analyzed cell (Figure 1) was chosen to have an architecture similar to the common Li-ion pouch cell.

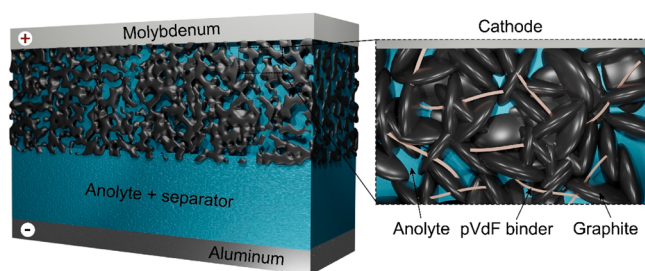


**Figure 1.** Schematics of the cell used in this work to evaluate the energy density of ADIBs.

Particularly, it consists of 20 double-side-coated graphite cathode layers on a Mo current collector, 20 layers of Mo cathode current collector foil, 40 layers of glass fiber separator, 20 layers of Al foil, and 2 layers of packaging foil. As shown in Figure S2, lower numbers of graphite cathode layers will yield significantly lower energy densities due to the increased ratio of inactive vs active battery components. The dimensions of the battery were 5.5  $\text{cm} \times 8.5 \text{ cm}$ . The thickness of the porous

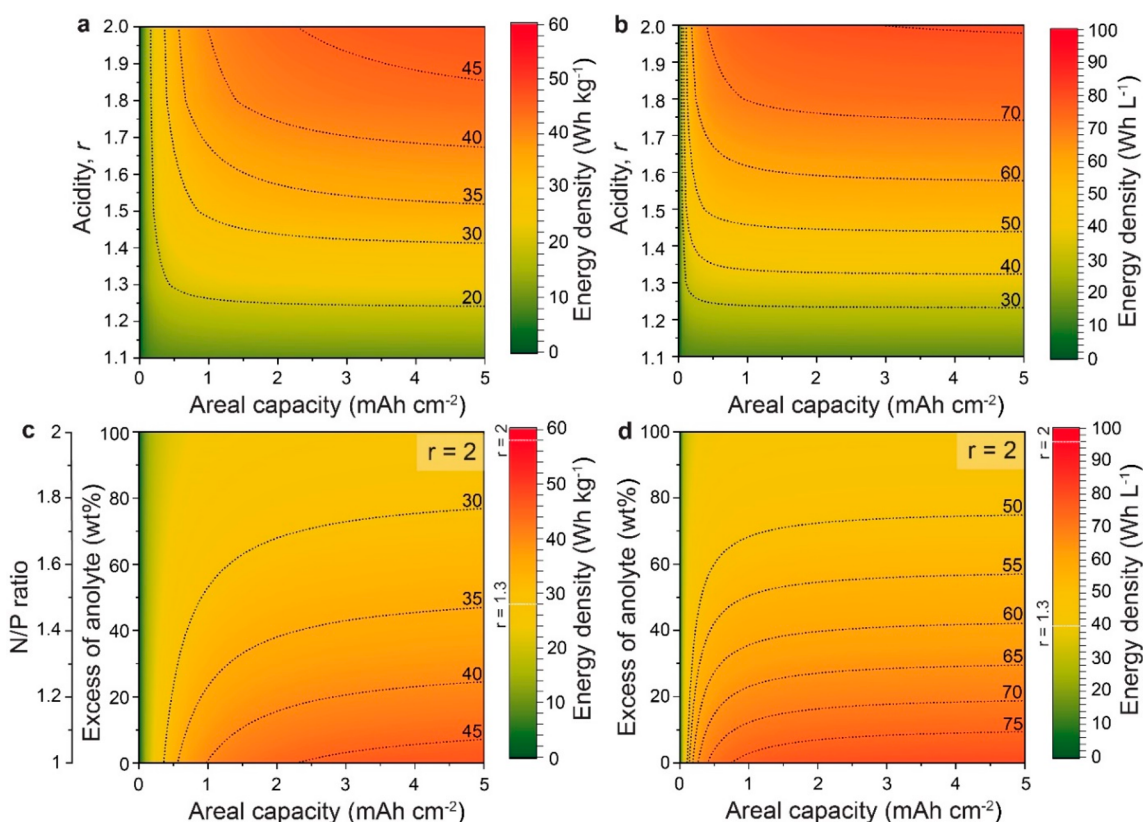
glass fiber separator was calculated from the total quantity of used anolyte minus the quantity present in the pores of cathode, considering the porosity of 81%. Further information on the thickness and density of the individual cell components can be found in Table S1 (see Supporting Information). The cell volume of the ADIB was calculated in the fully discharged state, i.e., the state in which the battery would be assembled. No kinetic or transport constraints were considered in these calculations.

Figure 2 summarizes the calculated achievable gravimetric and volumetric energy densities of ADIBs as functions of the areal capacity of the cathode, the anolyte acidity, and the excess of the anolyte. The profound effect of the anolyte acidity is seen when comparing  $r = 1.3$  and  $r = 2.0$ : gravimetric/volumetric energy densities rise from 23  $\text{Wh kg}^{-1}/37 \text{ Wh L}^{-1}$  to 40.2  $\text{Wh kg}^{-1}/76.6 \text{ Wh L}^{-1}$  (with 1  $\text{mAh cm}^{-2}$  graphite cathodes), respectively. This difference stems from the difference in capacities of the anolytes of low (19  $\text{mAh g}^{-1}$  and 25  $\text{mAh cm}^{-3}$  for  $r = 1.3$ ) and high acidity (49  $\text{mAh g}^{-1}$  and 69  $\text{mAh cm}^{-3}$  for  $r = 2.0$ ). Higher capacity corresponds to higher concentration of  $\text{Al}_2\text{Cl}_7^-$  ions, responsible for the electroplating of aluminum. Interestingly, the influence of the areal capacity of the graphite electrodes is significant only in the range of 0–1  $\text{mAh cm}^{-2}$ . For instance, the gravimetric/volumetric energy densities decrease only slightly from 47.4  $\text{Wh kg}^{-1}/80.8 \text{ Wh L}^{-1}$  to 40.2  $\text{Wh kg}^{-1}/76.6 \text{ Wh L}^{-1}$  (using an anolyte with  $r = 2$ ) when the areal capacity is decreased from 5 to 1  $\text{mAh cm}^{-2}$ .

On the contrary, further reductions of areal capacity to 0.5, 0.25, and 0.1  $\text{mAh cm}^{-2}$  lead to significant decreases of energy density to 33.8  $\text{Wh kg}^{-1}/72.0 \text{ Wh L}^{-1}$ , 25.6  $\text{Wh kg}^{-1}/64.3 \text{ Wh L}^{-1}$ , and 14.8  $\text{Wh kg}^{-1}/48.6 \text{ Wh L}^{-1}$ , respectively. Remarkably, this correlation between area capacity and energy density is vastly different for Li-ion batteries, where a drastic rise of the energy density persists to areal capacities of ca. 2  $\text{mAh cm}^{-2}$ . As apparent from Figure S3, this difference is mainly related to the large proportion of active materials of 66 wt% and 80 vol% (with 1  $\text{mAh cm}^{-2}$  graphite cathodes) in the total mass and volume of ADIBs, respectively. Therefore, the increase in the areal capacity of the electrodes, which leads to an increase in the fraction of active materials compared to the non-active materials, has a rather minor effect on the energy density at areal capacities of  $>1 \text{ mAh cm}^{-2}$ .

Importantly, our results show that the excess of anolyte has a drastic negative impact on the energy densities of ADIBs and should be minimized (see Figures 2c,d, S4–S7). For instance, the use of 50 wt% of excess anolyte (N/P ratio = 1.5,  $r = 2$ ) leads to a sharp decrease in energy density to 30.4  $\text{Wh kg}^{-1}/55.1 \text{ Wh L}^{-1}$  for a 1  $\text{mAh cm}^{-2}$  graphite cathode. Moreover, doubling the amount of anolyte (N/P ratio = 2,  $r = 2$ ) leads to nearly 40% lower values of gravimetric and volumetric energy densities (24.5  $\text{Wh kg}^{-1}$  and 43.1  $\text{Wh L}^{-1}$ ) of ADIBs.

Next, we analyze the volume change of ADIBs during cycling. In contrast to a rather small volume increase of graphite during intercalation of  $\text{Li}^+$  ions (ca. 10%), the volume of graphite can expand by up to 41% with intercalation of bulky  $\text{AlCl}_4^-$  anions.<sup>5</sup> Concomitantly, depending its acidity, also the volume of the anolyte can drastically change as well. For instance, in the case of a cell comprising  $\text{AlCl}_3\text{:EMIMCl}$  anolyte with  $r = 2.0$  (with N/P ratio = 1), its volume might decrease by up to 26%, corresponding to a complete depletion of  $\text{Al}_2\text{Cl}_7^-$  ions from the anolyte, reaching neutrality ( $r = 1$ ). The higher the molarity or acidity of the electrolyte, the greater



**Figure 2.** Calculated gravimetric (a, c) and volumetric (b, d) energy densities of ADIBs consisting of a graphite cathode and an  $\text{AlCl}_3/\text{EMIMCl}$  anolyte as a function of acidity (a, b) and excess (c, d) of the anolyte. The theoretical energy density values of the ADIBs, calculated based on the mass or volume of the graphite and anolyte active materials, are indicated as white lines ( $28 \text{ Wh kg}^{-1}$  and  $40 \text{ Wh L}^{-1}$  for  $r = 1.3$  and  $58 \text{ Wh kg}^{-1}$  and  $96 \text{ Wh L}^{-1}$  for  $r = 2.0$ ) on the energy density scales in (c) and (d).

is the volume change. To demonstrate the practical significance of volume variations in ADIBs during cycling, we calculated the volume changes of ADIBs based on anolyte with  $r = 2.0$  at different areal capacities of graphite cathode and amounts of anolyte. As shown in Figure S8, despite significant volume changes of the graphite cathode (41%) and anolyte (maximum 26% at N/P ratio of 1), the total volume of the cell changes only by up to 10 vol%. Smaller changes in the total volume are associated with a concomitant increase and decrease in the volumetric fraction of graphite cathode and anolyte from 16.5% to 25.6% and from 62.3% to 50.5%, respectively. The volumes of the other components of the cell remain the same, with the exception of the volume of the Al foil, the fraction of which increases only slightly from 2.7% to 3.5%. The changes in cell volume of the ADIBs with anolytes having  $r = 1.1$ – $2$ , higher N/P ratios, and graphite cathodes with different areal capacities ( $0$ – $5 \text{ mAh cm}^{-2}$ ) are shown in Figures S4–S7. Considering possible side reactions at the Al anode and Al dendrite growth,<sup>21</sup> the effects of varying the thickness of the Al anode ( $12$ – $100 \mu\text{m}$ ) were also analyzed (see Figures S9–S11).

## SUMMARY AND OUTLOOK

The number of reports on ADIBs has increased dramatically in recent years, mainly still focusing on the characteristics of individual battery components. Herein we analyzed the factors of critical importance for the development of commercial cells.

First, the anolyte acidity determines the gravimetric and volumetric capacity of the anolyte and therefore has a crucial influence on the energy density of ADIBs. The difference

between the energy densities of ADIBs with high- and low-acidity electrolytes can be as high as  $31 \text{ Wh kg}^{-1}$  ( $9 \text{ Wh kg}^{-1}$  for  $r = 1.1$  vs  $40 \text{ Wh kg}^{-1}$  for  $r = 2$ ) or  $63 \text{ Wh L}^{-1}$  ( $14 \text{ Wh L}^{-1}$  for  $r = 1.1$  vs  $77 \text{ Wh L}^{-1}$  for  $r = 2$ ), even though they are assembled with the same  $1 \text{ mAh cm}^{-2}$  graphite cathode.

Second, our calculations suggest that research efforts should focus on minimizing the excess quantity of the anolyte (with regard to theoretical) while maintaining the high rate capability of ADIBs. For instance, non-optimized cell architectures that use twice the theoretically required amount of anolyte (N/P ratio =  $2$ ,  $r = 2$ ) have ca. 40% lower energy density values. Notably, most reports on ADIBs do not indicate the used amount of anolyte.

Third, we found that the minimally required areal capacity of the cathode in ADIBs is  $1 \text{ mAh cm}^{-2}$ . Further increasing the areal capacity has a rather small effect on the energy density of ADIBs. Importantly, the majority of the reported ADIBs are assembled with relatively low loadings of  $<0.25 \text{ mAh cm}^{-2}$  and low anolyte acidity. This means that the practically achievable energy densities of such ADIBs cannot exceed  $10 \text{ Wh kg}^{-1}$ .

A fourth issue relates to the overall volume change of ADIBs, which can be as high as 10 vol%. Therefore, in addition to exploring new cathode materials and anolytes, researchers should focus on developing a radically new battery design for ADIBs that is very different from that used in commercial Li-ion batteries. So far, this aspect has hardly been discussed in the literature.

Kostiantyn V. Kravchuk [orcid.org/0000-0001-6149-193X](https://orcid.org/0000-0001-6149-193X)  
Maksym V. Kovalenko [orcid.org/0000-0002-6396-8938](https://orcid.org/0000-0002-6396-8938)



## ■ ASSOCIATED CONTENT

## SI Supporting Information

The Supporting Information is available free of charge at <https://pubs.acs.org/doi/10.1021/acsenerylett.2c02908>.

Table S1, parameters used for the calculations of energy density; Figures S1, S2, S4–S7, S9–S11, calculated gravimetric and volumetric energy densities of ADIBs; Figure S3, calculated mass and volume fractions of different battery components in the analyzed ADIBs; Figure S8, calculated volume change of ADIBs as a function of areal capacity of graphite cathode and anolyte excess (PDF)

## ■ AUTHOR INFORMATION

Complete contact information is available at:

<https://pubs.acs.org/10.1021/acsenerylett.2c02908>

## Notes

Views expressed in this Viewpoint are those of the authors and not necessarily the views of the ACS.

The authors declare no competing financial interest.

## ■ ACKNOWLEDGMENTS

This work was financially supported by the Empa project “GRAPHION”.

## ■ REFERENCES

- (1) Angell, M.; Zhu, G.; Lin, M.-C.; Rong, Y.; Dai, H. Ionic Liquid Analogs of  $\text{AlCl}_3$  with Urea Derivatives as Electrolytes for Aluminum Batteries. *Adv. Funct. Mater.* **2020**, *30* (4), 1901928.
- (2) Lin, M.-C.; Gong, M.; Lu, B.; Wu, Y.; Wang, D.-Y.; Guan, M.; Angell, M.; Chen, C.; Yang, J.; Hwang, B.-J.; et al. An Ultrafast Rechargeable Aluminium-Ion Battery. *Nature* **2015**, *520* (7547), 324–328.
- (3) Wang, D.-Y.; Wei, C.-Y.; Lin, M.-C.; Pan, C.-J.; Chou, H.-L.; Chen, H.-A.; Gong, M.; Wu, Y.; Yuan, C.; Angell, M.; et al. Advanced Rechargeable Aluminium Ion Battery with a High-Quality Natural Graphite Cathode. *Nat. Commun.* **2017**, *8* (1), 14283.
- (4) Chen, H.; Xu, H.; Wang, S.; Huang, T.; Xi, J.; Cai, S.; Guo, F.; Xu, Z.; Gao, W.; Gao, C. Ultrafast All-Climate Aluminum-Graphene Battery with Quarter-Million Cycle Life. *Sci. Adv.* **2017**, *3* (12), eaao7233.
- (5) Wang, S.; Kravchyk, K. V.; Krumeich, F.; Kovalenko, M. V. Kish Graphite Flakes as a Cathode Material for an Aluminum Chloride–Graphite Battery. *ACS Appl. Mater. Interfaces* **2017**, *9* (34), 28478–28485.
- (6) Foulletier, M.; Armand, M. Electrochemical Method for Characterization of Graphite-Aluminium Chloride Intercalation Compounds. *Carbon* **1979**, *17* (5), 427–429.
- (7) Elia, G. A.; Marquardt, K.; Hoepfner, K.; Fantini, S.; Lin, R.; Knipping, E.; Peters, W.; Drillet, J.-F.; Passerini, S.; Hahn, R. An Overview and Future Perspectives of Aluminum Batteries. *Adv. Mater.* **2016**, *28* (35), 7564–7579.
- (8) Ng, K. L.; Amrithraj, B.; Azimi, G. Nonaqueous Rechargeable Aluminum Batteries. *Joule* **2022**, *6* (1), 134–170.
- (9) Wu, M. S.; Xu, B.; Chen, L. Q.; Ouyang, C. Y. Geometry and Fast diffusion of  $\text{AlCl}_4$  Cluster Intercalated in Graphite. *Electrochim. Acta* **2016**, *195*, 158–165.
- (10) Bhauriyal, P.; Mahata, A.; Pathak, B. The Staging Mechanism of  $\text{AlCl}_4$  Intercalation in a Graphite Electrode for an Aluminium-Ion Battery. *Phys. Chem. Chem. Phys.* **2017**, *19* (11), 7980–7989.
- (11) Pan, C.-J.; Yuan, C.; Zhu, G.; Zhang, Q.; Huang, C.-J.; Lin, M.-C.; Angell, M.; Hwang, B.-J.; Kaghazchi, P.; Dai, H. An Operando X-Ray Diffraction Study of Chloroaluminate Anion-Graphite Intercalation in Aluminum Batteries. *Proc. Natl. Acad. Sci. U.S.A.* **2018**, *115* (22), S670–S675.
- (12) Elia, G. A.; Hasa, I.; Greco, G.; Diemant, T.; Marquardt, K.; Hoepfner, K.; Behm, R. J.; Hoell, A.; Passerini, S.; Hahn, R. Insights into the Reversibility of Aluminum Graphite Batteries. *J. Mater. Chem. A* **2017**, *5* (20), 9682–9690.
- (13) Manna, S. S.; Bhauriyal, P.; Pathak, B. Identifying Suitable Ionic Liquid Electrolytes for Al Dual-Ion Batteries: Role of Electrochemical Window, Conductivity and Voltage. *Mater. Adv.* **2020**, *1* (5), 1354–1363.
- (14) Zhao, Y.; VanderNoot, T. J. Electrodeposition of Aluminium from Nonaqueous Organic Electrolytic Systems and Room Temperature Molten Salts. *Electrochim. Acta* **1997**, *42* (1), 3–13.
- (15) Carlin, R. T.; Osteryoung, R. A. Aluminum Anodization in a Basic Ambient Temperature Molten Salt. *J. Electrochem. Soc.* **1989**, *136* (5), 1409.
- (16) Kravchyk, K. V.; Kovalenko, M. V. The Pitfalls in Nonaqueous Electrochemistry of Al-Ion and Al Dual-Ion Batteries. *Adv. Energy Mater.* **2020**, *10* (45), 2002151.
- (17) Elia, G. A.; Kyeremateng, N. A.; Marquardt, K.; Hahn, R. An Aluminum/Graphite Battery with Ultra-High Rate Capability. *Batter. Supercaps* **2019**, *2* (1), 83–90.
- (18) Kravchyk, K. V.; Kovalenko, M. V. Aluminum electrolytes for Al dual-ion batteries. *Commun. Chem.* **2020**, *3* (1), 120.
- (19) Kravchyk, K. V.; Seno, C.; Kovalenko, M. V. Limitations of Chloroaluminate Ionic Liquid Anolytes for Aluminum–Graphite Dual-Ion Batteries. *ACS Energy Lett.* **2020**, *5* (2), 545–549.
- (20) Shi, J.; Zhang, J.; Guo, J. Avoiding Pitfalls in Rechargeable Aluminum Batteries Research. *ACS Energy Lett.* **2019**, *4* (9), 2124–2129.
- (21) Zheng, J.; Bock, D. C.; Tang, T.; Zhao, Q.; Yin, J.; Tallman, K. R.; Wheeler, G.; Liu, X.; Deng, Y.; Jin, S.; et al. Regulating Electrodeposition Morphology in High-Capacity Aluminium and Zinc Battery Anodes Using Interfacial Metal–Substrate Bonding. *Nat. Energy* **2021**, *6* (4), 398–406.